

# RHIC Impedance

S.Y. Zhang

May 16, 2001

## Abstract

This report is the update of the RHIC impedance. Since the 1994 report, some components have been completed and added in the rings, and some devices and chambers have been changed. The resistive wall, space charge, broadband, and the low frequency impedances are included. The machine impedance measurement will take place, and the detailed review of the devices and chamber changes will be performed, in order to get a more reliable impedance estimate.

## 1 Introduction

The RHIC impedance has been reported in 1994 [1]. Since then, some components have been completed and added in the rings, and some devices and chambers have been changed. This report serves as the update of RHIC impedance, as we know. Based on this report, the impedance measurement will take place, and the detailed review of the devices and chamber changes will be performed, in order to get a more reliable impedance estimate.

The RHIC impedance is reviewed in the following categories.

1. Resistive wall impedance, which is of interest at very low frequency range.
2. Space charge impedance is frequency independent, which is negative inductive.
3. Broadband impedance, which is capacitive. Resonance frequency of broadband impedance is in a few  $GHz$ . Therefore, below the RHIC

cutoff frequency  $f_{cutoff} = 2.405c/2\pi b \approx 2.8 \text{ GHz}$ , this impedance can be seen approximately as an inductance. The bellows, steps, ports, etc., contribute mainly to the broadband impedance. The general relation between the longitudinal and transverse impedances,  $Z_T \approx (Z_\ell/n) 2R/\beta b^2$ , can be applied.

4. Low frequency impedance. Resonant modes of low frequency impedance are in tens to hundreds  $MHz$ . Therefore, the imaginary part of the impedance is not a pure inductance, and the real part will take place in the relevant frequency range. The low frequency impedance includes the BPM, the abort and injection kickers. The relation between the longitudinal and transverse impedance depends on the device.
5. Narrow band impedance is mainly from the RF cavities, the large steps and cavities of the vacuum chamber. This part will not be included in this report.

## 2 Resistive Wall Impedance

Assuming a smooth cylindrical vacuum chamber, the longitudinal and transverse resistive wall impedances are,

$$Z_\ell(\omega) = (\text{sgn}(\omega) + j) \frac{\beta Z_0 \delta_s}{2b} \frac{\omega}{\omega_0} \quad (1)$$

and

$$Z_T(\omega) = (\text{sgn}(\omega) + j) \frac{R Z_0 \delta_s}{b^3} \quad (2)$$

where  $Z_0$  is the impedance in free space,  $377 \Omega$ ,  $b$  is the radius of the vacuum chamber and  $R$  is the machine radius. The skin depth at the frequency  $\omega$  is defined as,

$$\delta_s = \sqrt{\frac{2\rho}{\mu_0 |\omega|}} \quad (3)$$

where  $\mu_0 = 4\pi \times 10^{-7} \text{ H/m}$  is the permeability of free space, and  $\rho$  is the resistivity of the vacuum chamber. For stainless steel we take  $\rho = 1 \times 10^{-6} \Omega m$  for warm region,  $\rho = 0.5 \times 10^{-6} \Omega m$  for cold region.

For the RHIC,  $R = 610.175 \text{ m}$ , and the beam pipe diameter is  $6.91 \text{ cm}$  for cold region of  $2955 \text{ m}$ ,  $12.28 \text{ cm}$  for warm region of  $879 \text{ m}$ . At the revolution frequency  $78.2 \text{ kHz}$ , the skin depth is  $\delta_s = 1.27 \text{ mm}$  and  $\delta_s = 1.80 \text{ mm}$  for cold and warm regions, respectively.

The longitudinal and transverse resistive wall impedances per ring at the revolution frequency are

$$Z_\ell(\omega_0) = 6.61(1 + j)\Omega \quad (4)$$

and

$$Z_T(\omega_0) = 5.86(1 + j)M\Omega/m \quad (5)$$

### 3 Space Charge Impedance

The longitudinal space charge impedance is,

$$Z_\ell(\omega) = -j \frac{gZ_0}{2\beta\gamma^2} \frac{\omega}{\omega_0} \quad (6)$$

where

$$g = 1 + 2 \ln \frac{b}{a} \quad (7)$$

For Gaussian distribution,  $a = \sqrt{2}\sigma$ , where  $\sigma$  is the transverse *rms* beam size.

The transverse space charge impedance is,

$$Z_T(\omega) = -j \frac{RZ_0}{\beta^2\gamma^2} \left( \frac{1}{a^2} - \frac{1}{b^2} \right) \quad (8)$$

The RHIC parameters are considered for the gold and proton beams at injection and storage. These are  $\gamma_{Auinj} = 10.5$ ,  $\gamma_{Austr} = 108$ ,  $\gamma_{pinj} = 31$ ,  $\gamma_{pstr} = 268$ . The beam sizes are  $a = \sqrt{2}\sigma = [0.26, 0.08, 0.22, 0.07] \text{ cm}$ . The longitudinal and transverse space charge impedances are

$$Z_\ell(\omega_0) = -j[10.5, 0.14, 1.37, 0.023]\Omega \quad (9)$$

and

$$Z_T(\omega_0) = -j[303, 29, 51, 5.9]M\Omega/m \quad (10)$$

The longitudinal impedance can be written as  $Z_\ell/n$ , with  $n = \omega/\omega_0$ . Thus, we have  $Z_\ell/n = Z_\ell(\omega_0)$ . Both  $Z_\ell/n$  and  $Z_T$  are negative inductive, and independent of the frequency.

## 4 Broadband Impedance

The broadband impedance comes from the bellows, steps, vacuum ports and valves. Many other machine devices, such as the scraper, collimator, beam detectors, also contribute partially to the broadband impedance.

Since the real part of these impedance rises only above the pipe cut-off frequency, therefore, it is negligible. In the following, only the imaginary part of the longitudinal impedance,  $Z_\ell/n$ , will be presented. The transverse impedance will be obtained by using

$$Z_T \approx \frac{2R}{\beta b^2} \left( \frac{Z_\ell}{n} \right) \quad (11)$$

The scaling rules for shielding and tapering used in this report are as follows.

- The shielded bellows have impedance reduction factor of 12 and 5, for longitudinal and transverse, respectively, according to the SSC study [2]. The RHIC measurement [3] shows a larger than a factor of 20 reduction for the longitudinal impedance. We take a factor of 10 reduction in the impedance estimate, with the consideration of the 2 mm step at the one end, and the imperfect finger contact on the other end, of the shielding.
- A taper length twice of the transition height reduces both longitudinal and transverse impedances by a factor of 2. A further extension to 10 times of the transition height reduces the longitudinal impedance by another 25%, and the transverse, 40% [4]. In general, we take a factor of 2 for the tapering reduction.
- For the BPM tanks, one end is tapered with a ratio of 2, and another end is not tapered. For single plane and dual plane BPMs with 70° striplines, the shielding ratio is 0.39 and 0.78. A factor of 2 reduction in the impedance is taken for the BPM tank steps.

### 4.1 Bellows

The bellows impedance is estimated using the following equation for each convolution [5],

$$\frac{Z_\ell}{n} = j\omega_0 \frac{Z_0}{2\pi bc} \left( wh - \frac{w^2}{2\pi} \right) \quad (12)$$

where  $w$  and  $h$  are the width and height of a pillbox.

- For the RHIC [6], there are 420 cold bellows at  $b = 3.46 \text{ cm}$ , each has 24 corrugations of depth  $h = 1.1 \text{ cm}$  and length  $w = 0.3 \text{ cm}$ . Now that 96 repaired bellows per ring are not shielded. We have the impedance for these bellows as,

$$\frac{Z_\ell}{n} = j0.207\Omega \quad (13)$$

For the shielded 324 bellows, taking a factor of 10 reduction, the impedance is,

$$\frac{Z_\ell}{n} = j0.070\Omega \quad (14)$$

- For about 308 warm bellows at  $b = 6.14 \text{ cm}$ , the typical corrugations number is 40, with the depth  $1.27 \text{ cm}$  and length  $0.32 \text{ cm}$ . The impedance of the 82 unshielded bellow is,

$$\frac{Z_\ell}{n} = j0.205\Omega \quad (15)$$

For the shielded 214 bellows, taking a factor of 10 reduction, the impedance is,

$$\frac{Z_\ell}{n} = j0.053\Omega \quad (16)$$

- For the 12 unshielded warm bellows at  $b = 12.7 \text{ cm}$ , there are 20 corrugations of depth  $1.9 \text{ cm}$  and length  $0.73 \text{ cm}$ . The impedance is,

$$\frac{Z_\ell}{n} = j0.024\Omega \quad (17)$$

- Total bellows are about 728 per ring. Unshielded 190 bellows have total impedance of  $j0.436 \Omega$ , and the shielded 538 bellows have impedance of  $j0.123 \Omega$ , which is taking a factor of 10 reduction. Total impedance is  $j0.559 \Omega$ .
- Resonant frequency and quality factor are estimated using [7],

$$f_R \approx \frac{c}{4(h+w)} \quad (18)$$

and

$$Q \approx \left(\frac{2}{\pi}\right)^2 \frac{b}{h} \quad (19)$$

For the bellows at  $b = 3.46 \text{ cm}$  and  $b = 6.14 \text{ cm}$ , we have  $Q = 1.5$  and  $1.9$ ,  $f_R = 6.2 \text{ GHz}$  and  $4.7 \text{ GHz}$ , respectively.

The bellows in a half sextant is shown in Table 1 and Table 2, where total number per ring is also listed. Situations at each straight section in the warm region are all different, and keep changing. A detailed review is needed to get a more precise count.

<i>Position</i>	<i>No.</i>	<i>Total</i>	<i>Shield</i>
IP	2	24	Yes
IP-DX	1	12	No
DX	1	12	No
DX-D0	1	12	No
DX-D0	1	12	Yes
D0	1	12	No
D0-Q1	1	12	Yes
Q1-Q2	1	12	Yes
Q2-Q3	1	12	Yes
Q3-W/B	1	12	No
W/B	6	72	Yes
W/B, Irregular		~70	Yes
W/B, Irregular		~10	No
W/B-DU3	1	12	No
DU3-Q4	1	12	No

Table 1, Warm Region Bellows

<i>Position</i>	<i>No.</i>	<i>Total</i>	<i>Shield</i>
Q4-Q5	1	12	Yes
Q5-D5X	1	12	No
D5X-Q6	2	24	No
Q6-D6	2	24	No
D6-Q7	1	12	No
Q7-DU7	1	12	No
DU7-Q8	1	12	No
Q8-D8	1	12	Yes
D8-Q9	1	12	Yes
Q9-Q21	24	288	Yes

Table 2, Cold Region Bellows

## 4.2 Steps

The impedance of a step can be estimated by using the equation,

$$\frac{Z_\ell}{n} = j\omega_0 \frac{Z_0 h^2}{4\pi^2 b c} \left( 2 \ln \frac{2\pi b}{h} + 1 \right) \quad (20)$$

and the difference between a step-up and a step-down is disregarded in this report.

- The aperture changes occur at the warm to cold transitions, near Q4 on either side of each IR. There are 16 such transitions, with  $b = 3.46 \text{ cm}$  to  $b_1 = 6.14 \text{ cm}$ . A ratio 5 tapering is applied. Taking a factor of 2 reduction, total impedance is,

$$\frac{Z_\ell}{n} = j0.012\Omega \quad (21)$$

- For total 246 BPMs in a ring, 192 BPMs are located in the cold region. There are total 384 steps from the pipe with  $b = 3.46 \text{ cm}$  to  $b_1 = 4.80 \text{ cm}$ , i.e.  $h = 1.34 \text{ cm}$ . Taking a factor of 2 reduction, this gives rise to

$$\frac{Z_\ell}{n} = j0.102\Omega \quad (22)$$

- For the 54 BPM in the warm region, there are total 108 steps from the pipe with  $b = 6.14 \text{ cm}$  and  $b_1 = 7.64 \text{ cm}$ , i.e.  $h = 1.5 \text{ cm}$ . Taking a factor of 2 reduction, this gives rise to

$$\frac{Z_\ell}{n} = j0.023\Omega \quad (23)$$

### 4.3 Ports

Impedance of a round vacuum pumping hole of radius  $b_{port}$  can be estimated by,

$$\frac{Z_\ell}{n} = j \frac{Z_0}{6\pi^2} \frac{b_{port}^3}{Rb^2} \quad (24)$$

- There are total 233 round vacuum pumping holes at the cold region, with  $2.2 \text{ cm}$  diameter. Taking  $b_{port} = 1.1 \text{ cm}$ , the total longitudinal impedance, including the 16 similar ports at the warm to cold transitions, is

$$\frac{Z_\ell}{n} = j0.003\Omega \quad (25)$$

- There are 36 ports at  $b = 6.14 \text{ cm}$  with  $12 \text{ cm}$  diameter, and these ports are shielded. Taking a factor of 10 reduction, we have

$$\frac{Z_\ell}{n} = j0.002\Omega \quad (26)$$

### 4.4 Valves

For a deep pillbox,  $h \sim b$ , the impedance is,

$$\frac{Z_\ell}{n} = j\omega_0 \frac{Z_0}{2\pi bc} \left( wb \ln\left(1 + \frac{h}{b}\right) - \frac{w^2}{2\pi} \right) \quad (27)$$

- There are 16 vacuum valves at  $b = 3.46 \text{ cm}$ . Let a valve be roughly described by a pillbox with  $w = 3.46 \text{ cm}$ , and  $h = 4 \text{ cm}$ . Taking a factor of 10 for the shielding, we have

$$\frac{Z_\ell}{n} = j0.004\Omega \quad (28)$$

- There are 44 vacuum valves at  $b = 6.14 \text{ cm}$ . Taking factor of 10 for the shielding, we have

$$\frac{Z_\ell}{n} = j0.005\Omega \quad (29)$$

## 4.5 Other chamber changes and devices

Many chamber changes and devices are not included. Following shows an incomplete list, these devices contribute completely and/or partially to the broadband impedance.

1. DX-D0 crotch. 2. DCCT. 3. Wall current monitors. 4. Schottky cavities. 5. Schottky pick-ups. 6. Transverse dampers. 7. Longitudinal dampers. 8. Bottom pick-up. 9. IPM. 10. Polarimeter. 11. AC dipole. 12. AC quadrupoles. 13. Scrapers. 14. Crystal collimator. 15. Beam dump chamber. 16. Roman pot detectors. 17. PLL kicker. 18. Tune meter kicker, ...

## 5 Low Frequency Impedance

The low frequency impedance comes mainly from the BPM, abort kicker, and injection kicker.

### 5.1 Beam position monitor

The longitudinal impedance of a pair of strip plates is,

$$Z_\ell = 2Z_c \left( \frac{\phi_0}{2\pi} \right)^2 \left( \sin^2 \frac{\omega\ell}{c} + j \sin \frac{\omega\ell}{c} \cos \frac{\omega\ell}{c} \right) \quad (30)$$

where  $\ell$  and  $\phi_0$  are the BPM length and subtends, and  $Z_c$  is the characteristic impedance of the stripline. The reactive part, for the frequency much smaller than  $f_R$ , can be estimated as,

$$\frac{Z_\ell}{n} = j \frac{2Z_c}{n} \left( \frac{\phi_0}{2\pi} \right)^2 \sin \frac{\omega\ell}{c} \cos \frac{\omega\ell}{c} \approx j 2Z_c \left( \frac{\phi_0}{2\pi} \right)^2 \frac{\beta\ell}{R} \quad (31)$$

The transverse impedance can be obtained using the Nassibian-Sacherer derivation from the longitudinal impedance of the displaced beam. For a pair of striplines, the impedance in the perpendicular direction is [8],

$$Z_T = \frac{R}{\beta b^2} \left( \frac{4}{\phi_0} \right)^2 \sin^2 \frac{\phi_0}{2} \left( \frac{Z_\ell}{n} \right) \quad (32)$$

In another direction,  $Z_T \approx 0$ .

If  $\phi_0$  is not large, the transverse impedance can be estimated as,

$$Z_T \approx \frac{4R}{\beta b^2} \left( \frac{Z_\ell}{n} \right) \quad (33)$$

In the RHIC, there are 174 single plane BPM in each ring, plus 72 dual plane BPMs that have 4 striplines. All striplines have the length  $\ell = 23$  cm, but the subtends is  $\phi_0 = 80$  degrees for 192 BPMs in the cold region, and  $\phi_0 = 70$  degrees for 54 BPMs in the warm region. The characteristic impedance of the stripline is  $Z_c = 50 \Omega$ .

For the low frequency,  $\omega \ll c/\ell$ , the longitudinal and transverse impedances can be estimated by (31) and (32). Thus, we have,

$$\frac{Z_\ell}{n} \approx j0.53\Omega \quad (34)$$

and

$$Z_T \approx j0.92M\Omega/m \quad (35)$$

## 5.2 Abort kickers

### 5.2.1 Transverse impedance

In a window frame lump magnet, the transverse impedance is dominated by the differential flux in the core induced by the beam position deviation. Neglecting the chamber effect, the conductor shielding effect, and the ferrite boundary effects, etc. this yields the transverse impedance [9],

$$Z_T = \frac{c\omega\mu_0^2\ell^2}{4a^2Z_k}\Omega/m \quad (36)$$

where  $\ell$  is the magnet length,  $2a$  is the inner height, and  $Z_k = j\omega L + Z_g$ , with  $L$  the magnet inductance, and  $Z_g$  the termination impedance.

The RHIC horizontal abort kicker has 5 window frame magnet units, the average length is  $\ell = 1.22$  m, and the average inner width is  $2b = 5.08$  cm, all have the same height  $2a = 7.62$  cm.

The magnet inductance of each unit is  $L = \mu_0 b\ell/a = 1.02 \mu H$ . The stray inductance is about  $L_{stray} = 0.6 \mu H$ . The PFN is located between the magnet and the charging circuits, consisted of 20 sections, with  $L_{pfn} = 0.15 \mu H$ , and  $C_{pfn} = 4.15$  nF.

Recent measurement [10] shows that with the PFN connected, the largest peak real part of the horizontal impedance is  $Z_T \approx 1.5 M\Omega/m$  at  $10 MHz$ , with the quality factor  $Q \approx 3$ . The resonance frequency is low, because the stray capacitance, the ferrite module sees, is quite large, about  $220 pf$ . Also, the imaginary part of both horizontal and vertical impedances is about  $j0.25 M\Omega/m$ , which are extended beyond  $100 MHz$ . The real part of the vertical impedance is, as predicted, not significant.

### 5.2.2 Longitudinal impedance

For the abort kicker, the transverse and longitudinal impedances are not related, because that the longitudinal impedance is dominated by the flux leakage in the window frame magnet.

Consider the beam passing through a ferrite ring with the outer and inner radii  $b_2$  and  $b_1$ . The inductance of the ferrite ring is

$$L = \frac{\mu_r \mu_0 \ell}{2\pi} \ln \frac{b_2}{b_1} \quad (37)$$

where  $\mu_r$  is the relative permeability. For CMD5005 used in the abort kicker,  $\mu_r \approx 1000$ . To reduce the massive ferrite loss, copper sheets are placed in the ferrite core as flux break.

Let the thickness of the copper sheet be  $\delta_{copper}$ , then the corresponding leakage is estimated as [11],

$$L_{leak} = 2 \frac{\mu_0 \ell}{2\pi} \ln \frac{\pi a}{2\delta_{copper}} \quad (38)$$

Taking  $\delta_{copper} = 1 mm$ ,  $2a = 7.62 cm$ , we get  $L_{leak} = 2.0 \mu H$  for  $\ell = 1.22 m$ , i.e. one magnet module. This is 2.5% of the flux generated without the copper sheet. If we take a 1% flux leakage around the copper sheet, the total inductance of 5 modules presented to the beam is  $L_m = 5 \mu H$ . Using

$$\frac{Z_\ell}{n} = j\omega_0 L_m \quad (39)$$

the equivalent longitudinal impedance is  $Z_\ell/n = j 2.5 \Omega$ .

The total abort kicker longitudinal impedance,  $Z_\ell/n$ , has a real part of about  $1.7\Omega$ , resonated at about  $18 MHz$ , with a quality factor of  $Q \approx 0.5$ .

## 5.3 Injection kicker

### 5.3.1 Longitudinal impedance

The RHIC injection vertical kicker is transmission line type with 4 units, each has a length of  $\ell = 1.1 \text{ m}$ . The magnet is C-shaped CMD5005 ferrite, with the inner width  $2b = 5.02 \text{ cm}$ , and the height  $2a = 4.84 \text{ cm}$ . The magnet inductance of each unit is  $L = \mu_0 b \ell / a = 1.43 \text{ } \mu\text{H}$ .

The longitudinal impedance of the injection kicker is quite different from the one of abort kicker. Firstly, for the C-magnet, the dominant factor in the window frame magnet, i.e., the flux leakage through the copper sheet, no longer exists. Secondly, for the travelling wave kicker, the transit factor has to be considered, which is represented by the transit factor  $k$ , defined as

$$k = \frac{\omega \mu_0 b}{Z_c a} \quad (40)$$

where  $Z_c$  is the characteristic impedance of the transmission line. It is shown in [12] that if both ends of the magnet winding circuits are terminated properly, then the longitudinal impedance is,

$$\frac{Z_\ell}{n} = \frac{\omega_0 Z_c}{4\omega} ((1 - \cos k\ell) + j(k\ell - \sin k\ell)) \quad (41)$$

In the RHIC injection kicker, however, one end of the winding is terminated, and other end is open. Therefore, together with correction coefficients obtained from the measurement, the impedance is better matched by [13],

$$\begin{aligned} \frac{Z_\ell}{n} = & \frac{\omega_0 Z_c}{2\omega} (0.12(3 - 4 \cos k\ell + \cos 2k\ell) \\ & + 0.18j(0.33k\ell + 1.34 \sin k\ell - 0.34 \sin 2k\ell)) \end{aligned} \quad (42)$$

This formulation gives rise to the real part peaked at  $10 \text{ MHz}$ , with  $Z_\ell/n = 0.4 \text{ } \Omega$ , and the imaginary part peaked at  $5 \text{ MHz}$ , with  $Z_\ell/n = j0.55 \text{ } \Omega$ . Above  $20 \text{ MHz}$  up to  $100 \text{ MHz}$ , real part of impedance approaches zero, while the imaginary part stays at  $Z_\ell/n = j0.2 \text{ } \Omega$ .

A separate measurement of the RHIC injection kicker [14], focusing on the high frequency range, shows that  $Z_\ell/n \approx j0.25 \text{ } \Omega$  up to  $1 \text{ GHz}$ .

### 5.3.2 Transverse impedance

Applying the scaling of

$$\frac{2R}{\beta b^2} \approx 2.1 \times 10^6 \quad (43)$$

where  $b = 2.5 \text{ cm}$  is used, the transverse impedance can be obtained from the longitudinal impedance in (42). The scaled transverse impedance is approximately agreeable to the recent measurement [15], which shows that the scaling can be applied in the case of one end of the winding is terminated, while another is open. In Table 3, the transverse impedance scaled from the longitudinal one is compared with the measurement result.

	Longitudinal	Transverse Scaled	Measured
<i>Real, max</i>	0.41, at 10 MHz	0.80, at 10 MHz	0.64, at 7 MHz
<i>Imag., max</i>	$j0.56$ , at 5 MHz	$j1.1$ , at 5 MHz	$j1.2$ , at < 5 MHz
<i>Real, 100MHz</i>	0	0	0
<i>Imag. 100MHz</i>	$j0.2$	$j0.42$	$j0.4$
<i>Unit</i>	$\Omega$	$M\Omega/m$	$M\Omega/m$

Table 3

It is interesting to note that the measured injection kicker horizontal impedance has small real part but a quite large imaginary part. Up to the measurement range of 100 MHz, the imaginary part is flat at  $j0.7 \text{ M}\Omega/m$ . It will be of interest to measure this imaginary impedance at higher frequency.

It is also noted that large impedance at the very low frequency, similar to the wall impedance, is observed in the measurement of both abort kicker and injection kicker. This impedance is proportional to  $1/\omega$ , unlike the wall impedance, which is proportional to  $1/\sqrt{\omega}$ . Interpolation from the measurement data shows that at the revolution frequency the abort kicker will have an impedance larger than the resistive wall of the entire ring. Below the revolution frequency, the contribution of this impedance is even larger. All of this was not reported in previous measurements and literature, and it will be further investigated.

Finally, the dielectric loaded traveling wave modules in the yellow ring have been replaced by the all-ferrite units, which is partially traveling wave

type. The impedance was also measured, it is about 20% larger than the traveling wave modules [15].

## 6 Summary

A summary of the RHIC impedance is shown in Table 4.

	$Z_\ell/n, im.$	$Z_\ell/n, re.$	$Z_T, im.$	$Z_T, re.$
<b>Resistive wall</b>	$j6.61, at \omega_0$	$6.61, at \omega_0$	$j5.86, at \omega_0$	$5.86, at \omega_0$
<b>Space charge</b>				
<i>Gold, inj/str.</i>	$-j10.5/ - j0.14$		$-j303/ - j29$	
<i>Proton, inj/str.</i>	$-j1.27/ - j0.023$		$-j51/ - j5.9$	
<b>Broadband</b>				
<i>Bellows</i>	$j0.559$		$j0.412$	
<i>Steps</i>	$j0.137$		$j0.101$	
<i>Ports and Valves</i>	$j0.014$		$j0.010$	
<i>Total</i>	$j0.710$		$j0.523$	
<b>Low frequency</b>				
<i>BPM, max</i>	$j0.53$	$0.38$	$j0.92$	$0.67$
<i>Abort kicker, max</i>	$j2.5$	$1.7$	$j2.0$	$1.5$
<i>Inj. kicker, max</i>	$j0.56$	$0.41$	$j1.1$	$0.80$
<b>Unit</b>	$\Omega$	$\Omega$	$M\Omega/m$	$M\Omega/m$

Table 4

The total RHIC longitudinal impedance is shown in Fig.1, in a frequency range from  $0.1 MHz$  to  $10 GHz$ , where the dominant components in the corresponding frequency range are indicated.

The total RHIC transverse impedance is shown in Fig.2, for horizontal and vertical, respectively. The part contributed mainly from the wall and BPM are well understood, the part contributed from the abort kickers is matched to the measurement data, but not finally addressed. The broadband impedance is not complete. A general broadband impedance with  $Z_\ell/n = j0.5\Omega$  is added in the figures to cover the devices not included in this report.

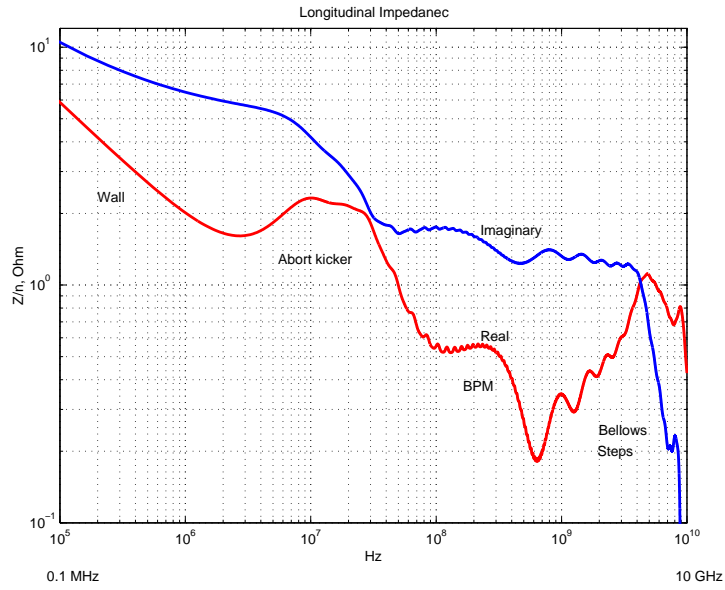


Figure 1: RHIC Longitudinal Impedance.

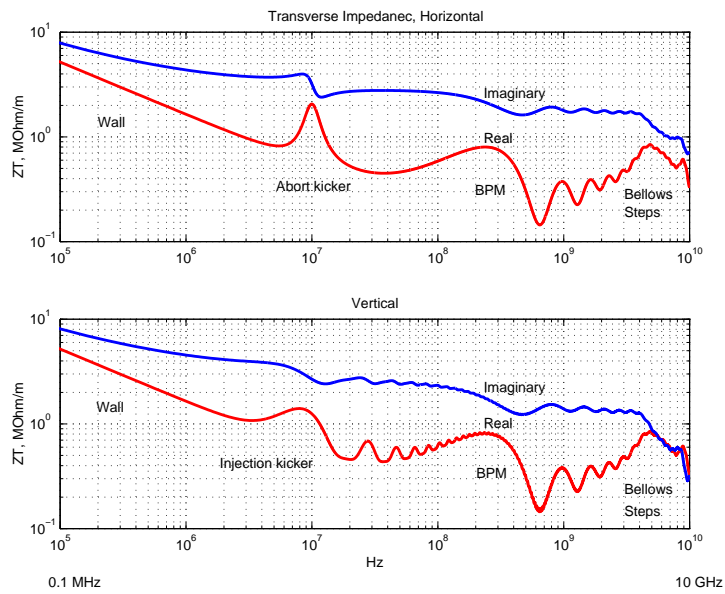


Figure 2: RHIC Transverse Impedance.

## References

- [1] S. Peggs and W.W. MacKay, RHIC/AP/36, Sep. 1994.
- [2] SSC CDR, SR-2020, March, 1986.
- [3] V. Mane, RHIC/AP/15, Jan. 1994.
- [4] M. D'yachkov and F. Ruggiero, LHC Project Report, 104, 1997.
- [5] S.S. Kurennoy, Particle Accelerators, Vol.45, p.95, 1994.
- [6] H.C. Hseuh, private communication.
- [7] G. Cavallari, Ph. Gayet, G. Geschonke, D. Kaiser, M. Jimenez, L. Vos, CERN SL-MD note 247, 1997.
- [8] R.E. Shafer, IEEE Trans. NS, Vol.NS-32,No.5, p.1933, 1985.
- [9] G. Nassibian and F. Sacherer, Nucl. Inst. Meth. Vol.159, p21, 1979.
- [10] H. Hahn, private communication.
- [11] G. Lambertson, Workshop on RHIC Performance, March, 1988.
- [12] K.Y. Ng, AIP Conference Proceedings, 184, 1989.
- [13] H. Hahn, AIP Conf. Proc. 496, 1999.
- [14] V. Mane, S. Peggs, D. Trbojevic and W. Zhang, PAC 95, p.3134, 1995.
- [15] H. Hahn and D. Davino, C-A/AP/45, March, 2001.